International Journal of Heat and Mass Transfer 52 (2009) 4519–4524

Contents lists available at ScienceDirect

International Journal of Heat and Mass Transfer

journal homepage: www.elsevier.com/locate/ijhmt

Operating limit of heat transport in two-phase thermosyphon with connecting pipe (heated surface temperature fluctuation and flow pattern)

Toshiaki Inoue [a,*], Masanori Monde [b]

[a] Department of Mechanical Engineering, Kurume Institute of Technology, 2228 Kamitsu, Kurume, Fukuoka 830-0052, Japan
[b] Department of Mechanical Engineering, Saga University, 1 Honjo, Saga 840-8502, Japan

ARTICLE INFO

Article history:
Received 4 July 2007
Received in revised form 28 January 2009
Accepted 13 March 2009
Available online 3 June 2009

Keywords:
Thermosyphon
Phase change
Flooding
Operating limit
Two-phase flow

ABSTRACT

An experiment on heat transport phenomena has been carried out in a two-phase thermosyphon with an adiabatic connecting pipe using water as the working fluid at atmospheric pressure. The thermosyphon has an upper liquid chamber and a lower vapor chamber, which are connected with an adiabatic pipe. A horizontal upward-facing heated surface is installed in the bottom of the lower vapor chamber.

The size of the connecting pipe is an inner diameter D_p = 2, 3, 4, 5, 6 and 8 mm and a length L = 250, 500 and 1000 mm. As the heat is supplied into the thermosyphon, the temperature of heated surface starts fluctuating at a heat flux at which unstable vapor–liquid counter current flow is generated in the connecting pipe. Bubbles at the upper end of the connecting pipe were photographed when the temperature fluctuation started. It was found that the heat flux at the onset of the temperature fluctuation increases with an increase in D_p and then can be predicted well by Eq. (1), which was derived based on the flooding velocity presented by Wallis [G.B. Wallis, One dimensional two-phase flow, McGraw Hill, New York, 1969], with C_w = 0.7 for D_p = 5, 6 and 8 mm. Furthermore, we clarified that the cause of this fluctuation comes from the inlet effect of the connecting pipe and we demonstrated this finding using a bell mouth, which was installed at either the bottom end or both ends of the connecting pipe.

1. Introduction

Cooling by boiling heat transfer using a two-phase thermosyphon is one of the methods available for heat dissipation. The operating limit of heat transport in the device should be clarified in order to make it operate stably. Many studies [1–14] have been performed on the operating limit of the thermosyphon with a uniformly heated pipe. An Eq. (1) is easily derived based on the flooding velocity as presented by Wallis [1]. This equation is for the mass flow rate of gas and liquid when flooding starts in an annular flow water–air system, in which air is supplied from the bottom end. Smirnov [4] and Imura et al. [5] proposed non-dimentional Eqs. (2) and (3) for critical heat flux (CHF) in the open two-phase thermosyphon, respectively. Monde et al. [6] derived an analytical Eq. (4) by discussing analytically the critical heat flux of the open two-phase thermosyphon and reported that the equation agreed well with the Smirnov [4] and the Imura et al. [5] correlations and CHF data from existing open two-phase thermosyphon. Monde et al. [7] measured the critical heat flux in a two-phase open thermosyphon with a pool and reported that their Eq. (4) predicted the CHF data with an error within ±30%. Furthermore, Monde and Mitsutake [8] confirmed that the CHF was enhanced by controlling the two-phase flow at the upper end of the open concentric thermosyphon, since the CHF is caused by a balance of momentum of the vapor and liquid there. Finally, Monde et al. [9] concluded that the critical heat flux, which might be related to an operating limit, was determined by a combination of constituting continuity and momentum equations and then envelope line of momentum equation, which is connecting maximum points determined by between superficial velocities of liquid. They show that their envelope method is just identical to the Katto method [10] and the Sudo method [11]

$$\Phi_f = C_w^2 B_0^{\frac{1}{4}} / \left\{1 + (\rho_v/\rho_L)^{\frac{1}{4}}\right\}^2 \quad (1)$$

$$\Phi_{CHF} = 0.65(\rho_L/\rho_V)^{0.1} \quad (2)$$

$$\Phi_{CHF} = 0.64(\rho_L/\rho_V)^{0.13} \quad (3)$$

$$\Phi_{CHF} = 0.67(\rho_L/\rho_V)^{1/8} \quad (4)$$

Fukano et al. [12] visually observed the aspect of vapor–liquid flow in the adiabatic section of a pipe and clarified the relation between the flow pattern and the operating limit in a closed two-phase thermosyphon with a uniform heated pipe. They informed that the operating limit appears due to a constraint of falling liquid to an evaporating section by the upward flow of vapor. Ueda and Miyashita [13] also clarified the mechanism of the operating limit based on

* Corresponding author. Tel.: +81 942 22 2345; fax: +81 942 22 7119.
E-mail address: inoue@cc.kurume-it.ac.jp (T. Inoue).

0017-9310/$ - see front matter © 2009 Elsevier Ltd. All rights reserved.
doi:10.1016/j.ijheatmasstransfer.2009.03.062

Nomenclature

A_h	area of heated surface
A_P	cross-sectional area of connecting pipe
B_O	bond number
C_w	friction coefficient on the wall
D_h	diameter of heated surface
D_P	inner diameter of connecting pipe
g	gravitational acceleration
H_{fg}	latent heat of evaporation
L_P	length of connecting pipe
m_V, m_L	mass flow rate of vapor and liquid, respectively
q_f	heat flux at onset of temperature fluctuation of the heated surface
t	time
T	temperature
ΔT_{sat}	wall superheat
δ	water level
δ^*	water level at onset of heated surface temperature decrease
ρ_L, ρ_V	density of liquid and vapor, respectively
σ	surface tension
Φ_f	non-dimensional heat flux

visual observation of flow state in an adiabatic section using closed two-phase thermosyphon with a uniform heated pipe. They concluded that a vapor plug holds up the liquid slug intermittently and brings about a periodic liquid circulation in the adiabatic section. Therefore, the operating limit seems to be caused by partial dry-out of the heated surface resulting from a periodical restriction of the liquid rate flowing down to the evaporator section. Finally, Koizumi et al. [14] also reported that dry-out was observed near the exit end of the heating section under an annular flow state in a two-phase natural circulation system.

As above-mentioned, most of studies related to the operating limit have been performed for the thermosyphon that operates under the condition that the adiabatic pipe diameter is the same as the heated pipe one.

The present thermosyphon has a large lower chamber where the heated surface is located in the bottom, in which a couple of liquid is evaporated on the upward heated surface. The thermosyphon may be widely used as a midget cooling system by a two-phase natural circulation. How the connecting conditions between the vapor chamber and the adiabatic section and between the liquid chamber and the adiabatic section influence the flow in the adiabatic pipe is of importance in determining the operating limit of the present thermosyphon. In order to clarify this effect on the operating limit, we install the bell mouth on the ends of the adiabatic connecting pipe. We focus on the heat flux when the temperature of the heated surface started fluctuating, and simultaneously observed a flow aspect inside the adiabatic pipe and bubble emission into the condensation section at the upper end of the pipe. Also, we discuss the relationship between the temperature fluctuation and the bubble emission and the effect of the inner diameter and length of the connecting pipe on the flow pattern and the heat flux. Furthermore, we find that the bell mouth at the bottom of the adiabatic pipe improves the heat flux at the onset of the temperature fluctuation and the bell mouth at the top of the pipe has no effect on the improvement.

2. Experimental apparatus and procedure

2.1. Experimental apparatus

Fig. 1 shows a schematic of our experimental apparatus. It consists of a vapor chamber (evaporation section), an insulated connecting pipe (adiabatic section) and a liquid chamber (condensation section). The details of the evaporation section are illustrated in Fig. 2. An horizontal upward-facing heated surface ① of copper is located in the bottom of the lower vapor chamber. Its size is D_h = 25 mm in inner diameter and L_h = 50 mm in length. The size of the upper liquid chamber is 105 mm in inner diameter and 390 mm in length. The filled water is kept at the level of about 250 mm during the experiment and is sufficient to operate the thermosyphon. Heat is supplied through a copper block ② with an electric heater ③. A Bakelite insulator is installed around the copper block to prevent heat loss to surroundings. Three thermocouples are inlaid along the center and their locations are 1.3 (T_1), 5.7 (T_2) and 11.4 mm (T_3) from the heated surface as shown in Fig. 2. Surface temperature and heat flux are calculated using these temperature measurements. An auxiliary heater ⑧ and a condenser ⑦ are installed in the condensation section to maintain the saturation condition of 98–100 °C at 0.1 MPa. The vessel of the condensation section is made of transparent polycarbonate to allow observation of bubble emission. We can observe a flow aspect inside the connecting pipe through a glass pipe ⑥ located as shown in Fig. 1 in the pipe of L_P = 250 mm.

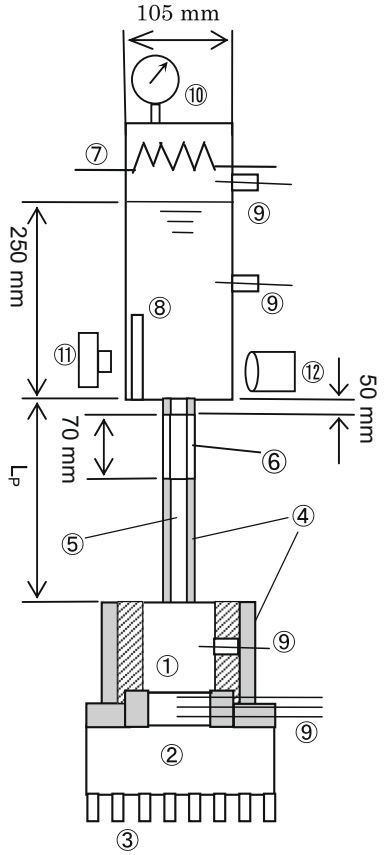

Fig. 1. Experimental apparatus. ① Heated surface, ② copper block, ③ heater, ④ insulator, ⑤ connecting pipe, ⑥ view glass pipe, ⑦ condenser, ⑧ auxiliary heater, ⑨ thermocouples, ⑩ pressure gauge, ⑪ camera, ⑫ high-speed stroboscope.

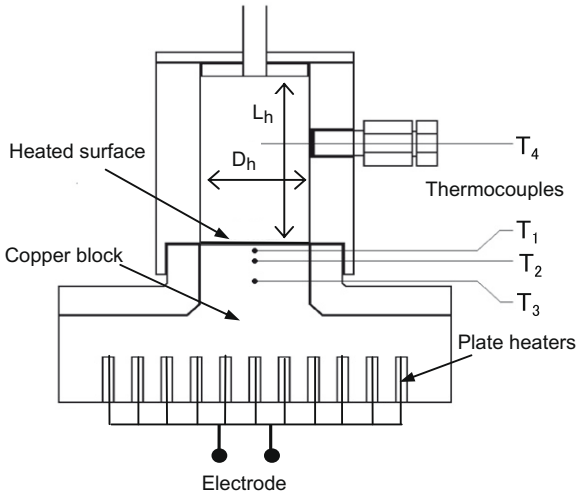

Fig. 2. Cross-sectional view of the copper block.

Fig. 3 shows the three kinds of connecting pipes and bell mouths that were used in the experiment. The first one has no bell mouth, the second one has a bell mouth placed at the bottom end and the third one has bell mouths at both ends.

2.2. Experimental procedure

We increased the heat flux to the heated surface in a stepwise manner within 5% increase per step, while maintaining the water saturation condition. Therefore, measurement error of the heat flux, q_f, at the onset of the temperature fluctuation is within 5%. We measured heat flux and surface temperature, after steady state was confirmed at each heat flux. We finished the experiment when the measured temperature started fluctuating. The experiment was first carried out without the bell mouth, then with the bell mouth at the bottom and with the bell mouth at both ends last. In the experiment, the inner diameter of the pipe used was D_P = 2, 3, 4, 5, 6 and 8 mm and its length was L_P = 250, 500 and 1000 mm.

2.3. Measurement error and heat loss

Heated surface temperature and heat flux were calculated using measured temperatures T_1 and T_2 shown in Fig. 2. The values of the temperature and the heat flux agreed with the calculated ones using the temperatures T_1 and T_3. It was confirmed that the three measured temperatures for each heat flux prior to onset of the temperature fluctuation could be depicted graphically as a straight line. The difference between the temperature T_1 and the heated surface temperature T_w varied from 0.5 to 1.0 °C depending on the heat flux. Here, the time constant of the thermocouples is a few seconds for a sheath diameter of 1 mm and wire diameter of 0.15 mm.

Monde and Katto [15] collected vapor generated on the heated surface and calculated the corresponding amount of heat transfer. They reported that the heat loss to the surroundings was 10% of the electric input power. The heat loss was about 15% of the input power at the onset of the temperature fluctuation in the present experiment.

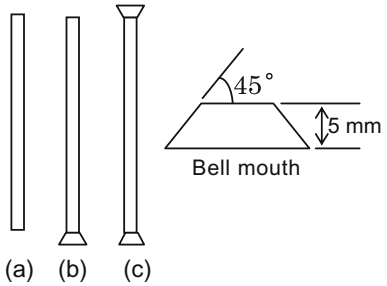

Fig. 3. Pipe without and with bell mouth and size of bell mouth.

3. Experimental results

3.1. Boiling curve

Fig. 4 shows an example of a boiling curve. Black symbols correspond to the onset of the temperature fluctuation and the solid line is the Stephan and Abdelsalam [16] correlation. The wall superheat is larger than their predicted value by 24%. The discrepancy is mainly caused by the difference of the surface factor of the heated surface. The slope between the correlation and the measured values is almost the same. Therefore, normal boiling is continuing on the heated surface, which means that there is sufficient liquid on it until the T_f point.

3.2. Fluctuation of measured temperature and flow pattern

The measured temperature, T_1, did not monotonically rise, but fluctuated at given heat flux, since the liquid is discontinuously supplied from the upper liquid chamber to the lower chamber.

Fig. 5 shows the occurrence of the T_1 temperature fluctuation at the heat flux of q = 38.1 kW/m^2 for D_P = 3 mm, and of q = 199 kW/m^2 for D_P = 6 mm. For the case of D_P = 3 mm, the temperature starts gradually decreasing and then suddenly rises to the temperature before it started decreasing. After the recovery of the temperature, the gradual temperature decrease starts again. This temperature change is repeated. Fig. 5(a) shows one frame for the temperature fluctuation. This type of fluctuation is observed for D_P = 2, 3 and 4 mm. It takes a long time for the next fluctuation to occur for D_P = 2, 3 and 4 mm, since the heat flux at the onset of the temperature fluctuation is relatively small so that the time until the liquid supplied is consumed becomes longer.

On the other hand, for the case of D_P = 6 mm, the time for the consumption of the liquid supplied becomes shorter, so that the cycle of the temperature fluctuation also becomes shorter. This type of fluctuation can be observed for D_P = 5, 6 and 8 mm.

Fig. 6 shows a flow situation during the temperature change at the heat flux of 85.3 kW/m^2 for D_P = 4 mm. The successive numbers on the photographs follow those on the temperature chart. The

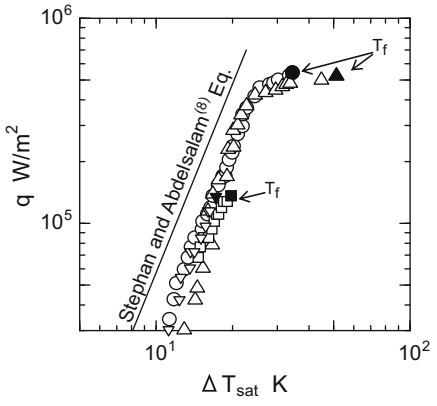

Fig. 4. Boiling curve. ●, ▲, ■, ▼: Onset of temperature fluctuation. L = 500 mm (D_P = 8 mm (○); D_P = 5 mm (□)). L = 1000 mm (D_P = 8 mm (△); D_P = 5 mm (▽)).

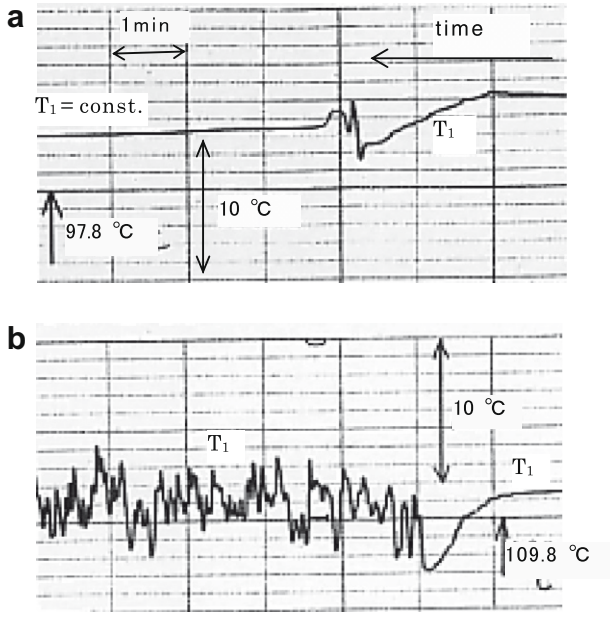

Fig. 5. T_1 temperature fluctuation. (a) q = 38.1 kW/m^2, D_p = 3 mm, L = 1000 mm. (b) q = 199 kW/m^2, D_p = 6 mm, L = 1000 mm.

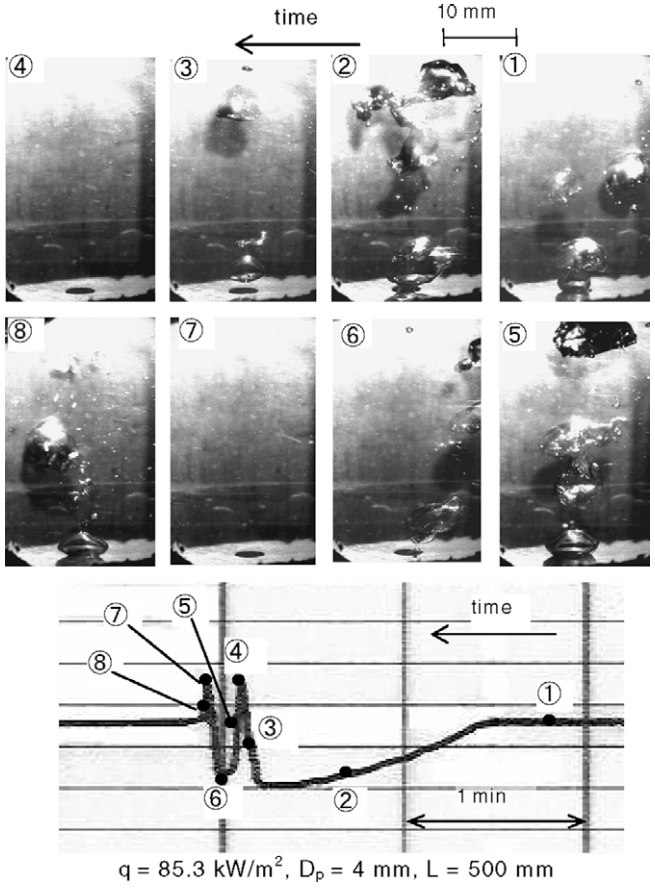

Fig. 6. Bubble emission and T_1 temperature fluctuation.

photos ① and ② show the successive bubbles, during which the temperature is gradually decreasing. This fact means that water is being consumed by evaporation and a lot of vapor is being generated. In addition, for this duration, water supply through the pipe from the top may be constrained by the vapor flow in the pipe. Then the consumption of water by evaporation may be larger than the supplied water, making the water level on the heated surface lower. The temperature decrease is due to the enhancement of heat transfer by evaporation of the thin liquid film. It may be worth mentioning that according to Nishikawa et al. [17], the wall superheat decreases due to the enhancement of evaporation for low water levels below 5 mm at a heat flux of $q \leqq 65$ kW/m^2. In the time between photos ② and ③, water is totally consumed and then the surface temperature starts increasing. After the heated surface becomes dry, no vapor is generated so that there is no constraint for water falling down in the pipe. Water starts to be fed to the heated surface again, but water does not yet reach the heated surface at the time corresponding to number ③. The water reached the heated surface again at the time corresponding to number ④, where the temperature starts decreasing. Just after this point, a large amount of the vapor is emitted due to intense evaporation as shown in photograph ⑤. A large amount of the generated vapor restricts the supply of water again. The transient temperature change continues from ④ to ⑧. It was found that the above- mentioned changes are periodically repeated for D_P = 2, 3 and 4 mm.

Fig. 7 illustrates the model for the flow pattern during the temperature fluctuation. It is based on both the temperature fluctuation and the bubble aspect. The successive numbers in Fig. 7 correspond to those on the photograph and the temperature change in Fig. 6. It is supposed that the flow pattern of bubbles in the pipe is slug flow as shown in Fig. 7, since bubbles are intermittently emitted as shown in the photographs of Fig. 6. In the case of flow pattern number ① in Fig. 7, the heated surface temperature is kept stable as shown in Fig. 6, although the flow rate of water is less than that of vapor, namely $m_L < m_v$. In other words, enough water exists on the heated surface to make boiling continuous. In the case of flow pattern number ② in Fig. 7, water on the heated surface is not hot enough for the boiling, so that evaporation occurs. According to Fig. 5, it takes about 90 s for water to be totally consumed at q = 85.3 kW/m^2. We tentatively calculated the water level for that condition to be 3.5 mm. We may conclude that evaporation occurs for low water levels during this period from photographs ① to ②.

Just after the heated surface is dried, water is supplied again. However, the surface is still dry, since it takes a few seconds for water to reach the surface. The heated surface is cooled down, after the surface is wetted again. The first contact of water produces

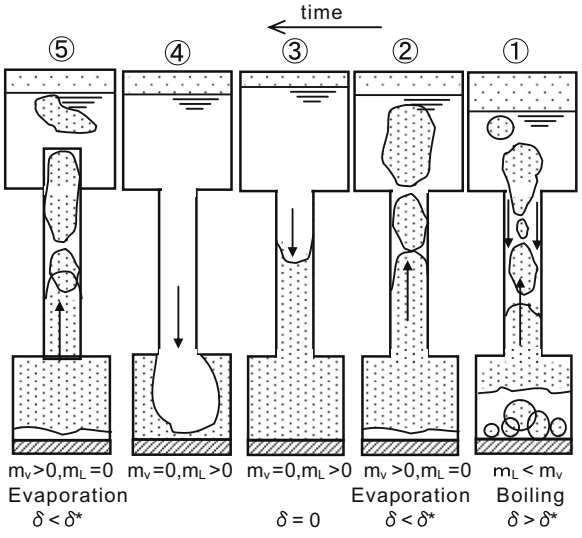

Fig. 7. Model of flow pattern in D_p = 2, 3 and 4 mm.

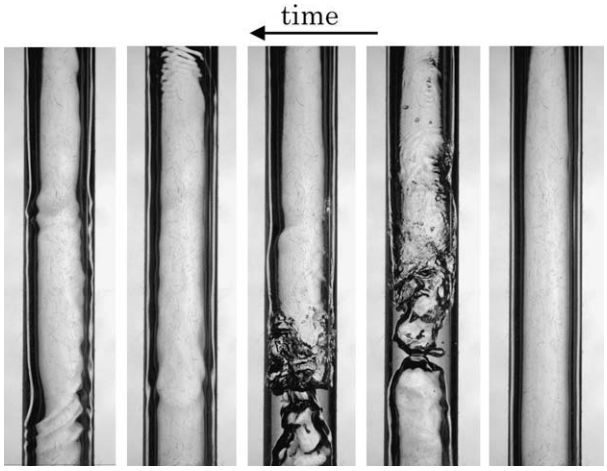

Fig. 8. Flow aspect during T_1 temperature fluctuation in $D_P = 6$ mm (Successive times at a period of 2 min).

vigorous boiling and water splashes out. The second temperature rise in Fig. 6 may result from the dryness of the surface due to the splashing out of the water. However, scattered water stays in the evaporation section and wets the heated surface again. It is probable that the heated surface temperature fluctuates due to repeat of the above-mentioned flow behavior.

Fig. 8 shows a flow aspect inside the adiabatic pipe during a temperature fluctuation in $D_P = 6$ mm. It is observed in Fig. 8 that a vapor plug is incidentally formed in the annular flow and holds up a liquid slug.

3.3. The effect of the size of the connecting pipe on the heat flux, q_f

Fig. 9 illustrates the effect of the inner diameter and the length of the connecting pipe on the heat flux, q_f, at the onset of the fluctuation. The heat flux always increases for any pipe length with an increase in the inner diameter of the pipe. The effect of the pipe length on the heat flux may be relatively small, although the pipe length of $L_P = 250$ mm makes the heat flux slightly larger than that

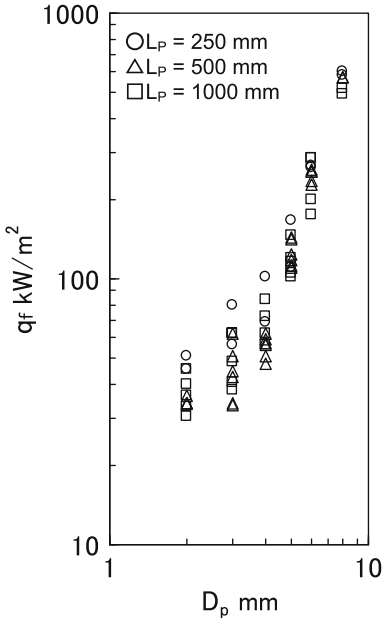

Fig. 9. The effect of pipe diameter and length on heat flux, q_f.

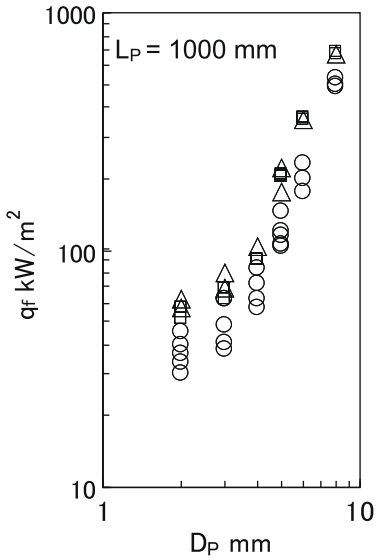

Fig. 10. The effect of bell mouth. (○) Without bell mouth. (▲) With bell mouth at bottom end. (□) With bell mouth at both ends.

of $L_P = 500$ and 1000 mm. The effect of the pipe length on the heat flux may be related to the flow situation at the top of the pipe.

3.4. The effect of the bell mouth

Fig. 10 shows the effect of the bell mouth on the heat flux, q_f. It is found that q_f is increased by the bell mouth installed in the bottom end of the pipe for any diameter of the pipe. While the bell mouth at the top of the pipe has no effect on the enhancement of the heat flux. This fact implies that the bell mouth controls the vapor flow at the entrance of the pipe. Remembering the envelope method proposed by Monde et al. [9], one notices that the momentum equation includes a wall shear stress obtained experimentally. The bell mouth attached at the entrance probably makes the wall shear stress reduce, resulting into an enhancement of the operating limit.

3.5. Relationship between heat flux at the onset of the fluctuation and flooding

We compared the heat flux, q_f, with the Eq. (1) for flooding as shown in Fig. 11, since the temperature fluctuation occurs due to unstable counter flow of vapor–water in the pipe. The Imura et al. Eq. (3) and the Monde et al. Eq. (4) are also shown in Fig. 11. Here Φ_f is a non-dimensional value defined by Eq. (5).

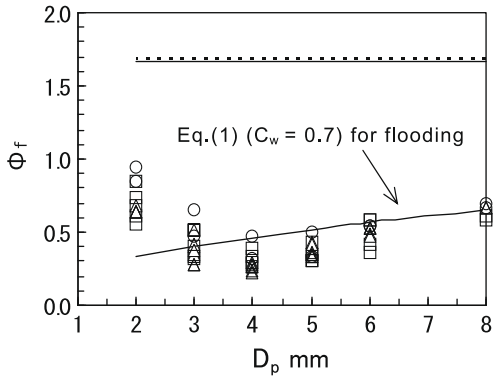

Fig. 11. Relationship between Φ_f and D_p. (—) Imura's Eq. (3) for CHF. (– – – –) Monde's Eq. (4) for CHF.

$$\Phi_f = \left(\frac{A_h}{A_p}\right)\left\{\frac{q_f}{\rho_v H_{fg}[\sigma g(\rho_L-\rho_v)/\rho_v^2]^{1/4}}\right\} \quad (5)$$

The value of the Φ_f gained by the present experiment is about one third of values predicted by Eqs. (3) and (4) as shown in Fig. 11. This is probably because the superficial velocity of generated vapor becomes the highest at the upper end of the pipe, resulting into occurrence of the flooding there for the case of a uniformly heated pipe, which is their system. The present system does not supply any vapor into the connecting pipe and keeps the superficial velocity constant. Ueda and Miyasita [13] discussed that CHF data obtained by Imura et al. [5] using the open system were larger than those obtained using the closed system. Koizumi et al. [14] also reported that CHF in a two-phase natural circulation system is extremely larger than that in the closed system. As our experimental system may be closer to the closed system, the heat flux, q_f, is lower than that from Eqs. (3) and (4).

The Eq. (1), which is derived for two-phase annular flow in water–air system in which air is fed into the pipe from the bottom end, mostly agrees with the experimental data for the pipe of D_P = 5, 6 and 8 mm. Here, the Eq. (1) has C_W = 0.7, which is the lower limit of the friction coefficient. Therefore, it is supposed that there is annular flow inside the pipe and it is disturbed anywhere in the adiabatic pipe by flow condition at the vapor entrance, by which the flooding condition is reached anywhere in the pipe and the T_1 temperature fluctuation was lasting. The bell mouth seems to suppress the turburence of the vapor flow.

On the other hand, the experimental data are extremely different from Eq. (1) for D_P = 2, 3, and 4 mm. Here, we put D_P = 4 mm into the grope of D_P = 2 and 3 mm, since the type of T_1 temperature fluctuation was in the category of (a) in Fig. 5. This is probably due to that the flow pattern for D_P = 2, 3 and 4 mm is not annular flow, but slug flow as shown in Figs. 6 and 7 and Eq. (1) was derived in annular flow. The heat flux at the onset of fluctuation becomes extremely higher than the prediction by Eq. (1) for D_P = 2 mm. The cause of this is not clear, even though it may be related to the flow condition at the bottom end of the pipe.

4. Conclusions

We have measured the heat flux, q_f, at the onset of the T_1 temperature fluctuation in a two-phase thermosyphon with the connecting pipe and simultaneously we visually observed the bubble emission aspect into water at the upper end of the pipe. We have clarified the effect of the inner diameter and length of the pipe on the heat flux and the flow pattern and we can summarize it as follows:

(1) The heat flux, q_f, increases with an increase in the inner diameter of the pipe.
(2) The heat flux is enhanced by the bell mouth installed at the vapor entrance.
(3) The heat flux can be predicted well by the Eq. (1) for the pipe of D_p = 5, 6 and 8 mm.
(4) There are two different flow patterns when the operating limit appears.

References

[1] G.B. Wallis, One Dimensional Two-Phase Flow, McGraw Hill, New York, 1969. pp. 338.
[2] C.L. Tien, K.S. Chung, Entrainment limits in heat pipes, AIAA J. 17 (1979) 643–646.
[3] H. Ngyuen Chi, M. Groll, Entrainment or Flooding Limits in a Closed Thermosyphon, Advances in Heat Pipe Technology, Pergamon Press, 1981. pp. 147–162.
[4] Y.L. Smirnov, Critical heat flux in flooding in vertical channels, Heat Transfer Sov. Res. 16 (3) (1984) 19–24.
[5] H. Imura, K. Sasaguchi, H. Kozai, S. Numata, Critical heat flux in a closed two-phase thermosyphon, Int. J. Heat Mass Transfer 26 (1983) 1181–1188.
[6] M. Monde, S. Mihara, T. Inoue, An analytical study of critical heat flux of a two-phase thermosyphon, Trans. Jpn. Soc. Mech. Eng. Ser. B 59 (560) (1993) 1258–1264.
[7] M. Monde, S. Mihara, Y. Mitsutake, Experimental study of critical heat flux of open two-phase thermosyphon, Trans. Jpn. Soc. Mech. Eng. Ser. B 62 (594) (1996) 729–733.
[8] M. Monde, Y. Mitsutake, Enhancement of CHF in open thermosyphon with heated bottom chamber, Int. J. Heat Mass Transfer 43 (2000) 3341–3346.
[9] M. Monde, Y. Mitsutake, A. Kurihara, S. Mihara, Analytical study of critical heat flux in two phase thermosyphon (relationship between maximum falling liquid rate and critical heat flux), JSME Int. J. Ser. B 39 (4) (1996) 768–779.
[10] Y. Katto, Limit conditions of steady-state countercurrent annular flow and the onset of flooding with reference to the CHF of boiling in a bottom-closed vertical tube, Int. J. Multiphase Flow 20 (1994) 45–61.
[11] Y. Sudo, Analytical study of critical heat flux under countercurrent flow limitation in vertical channels, Trans. JSME Ser. B 60 (580) (1994) 4222–4228.
[12] T. Fukano, K. Kadoguchi, H. Imuta, Experimental study on the heat flux at the operating limit of a closed two-phase thermosyphon, Trans. Jpn. Soc. Mech. Eng. Ser. B 53 (487) (1987) 1065–1071.
[13] T. Ueda, T. Miyashita, On the performance limit of closed two-phase thermosyphons, Heat Transf. Jpn. Res. 20 (6) (1991) 602–617.
[14] Y. Koizumi, T. Yoshinari, T. Ueda, T. Matsuo, T. Miyashita, Study on dry-out heat flux of two-phase natural circulation, Trans. Jpn. Soc. Mech. Eng. Ser. B 60 (570) (1994) 545–551.
[15] M. Monde, Y. Katto, A study of burnout mechanism in saturated forced convection boiling with impinging jet (the first report, characteristics of bubble behavior), Trans. Jpn. Soc. Mech. Eng. Ser. B, vol. 43, No. 373, Series 2, (1977) 3399–3407.
[16] K. Stephan, M. Abdelsalam, Heat-transfer correlations for natural convection boiling, Int. J. Heat Mass Transfer 23 (1980) 73–87.
[17] K. Nishikawa, H. Kusuda, K. Yamasaki, K. Tanaka, Nucleate boiling at low liquid levels, Bull. JSME 10 (1967) 328.